Localized Charge Distributions. I. General Theory, Energy Partitioning, and the Internal Rotation Barrier in Ethane[1]

Walter England* and Mark S. Gordon

Contribution from the Department of Chemistry and Institute for Atomic Research, Iowa State University, Ames, Iowa 50010. *Received October 15, 1970*

Abstract: Energy-localized orbitals are used to define localized distributions of positive charge and an energy partitioning of *ab initio* molecular orbital wave functions in the localized representation is derived. This partitioning is specialized to the INDO approximation using results from Ruedenberg's theory of chemical bonding. An interpretation is given for the internal rotation barrier in ethane with particular emphasis on the effects of geometry optimization. It is found that the origin of the barrier can be ascribed to one-electron interference energy differences among vicinal hydrogens, and that these are related to hyperconjugate effects.

The algorithm for energy localization reported by Edmiston and Ruedenberg[2] provides a computational method for the transformation of canonical molecular orbitals[3] to orbitals which are equivalent in a quantum mechanical sense and give rise to individual, chemically familiar electron distributions. These are the localized molecular orbitals which provide, *e.g.*, lone pairs and bond orbitals in a nonarbitrary way within the mathematically tractable molecular orbital theory.

In the present paper, each localized orbital is used to define a localized distribution of nuclear charge which, though arbitrary, is physically sensible. Together, the localized orbital and its induced positive distribution are called a localized charge distribution. The general form of the latter with a corresponding energy partitioning and interpretation for closed-shell wave functions is described in section I. In section II this partitioning is specialized to the semiempirical INDO method,[4] and in section III an interpretation is given using results from Ruedenberg's description of chemical bonding.[5]

A clear understanding of the barrier to internal rotation in ethane has been a long-standing problem in quantum chemistry. Part of the elusive nature of barrier understanding is undoubtedly due to the fact that energy differences, often rather small and numerous, are involved. The work of Epstein and Lipscomb[6] makes this elusiveness especially clear. We feel, therefore, that one must be particularly attentive to physical, or qualitative, ideas which may be used to support the conclusions obtained from any calculations.

Although it has recently been shown[6-9] that energy optimization of the geometry can have a considerable effect on internal rotation barriers, it is usual to allow only the dihedral angle to vary.[10-17] As a result, most conclusions concerning the barrier in ethane begin with the assumption that the nuclear repulsions (as well as electron repulsions) are much larger in the eclipsed rotamer. In section IV of this paper, the partitioning mentioned in the preceding paragraph is applied to the INDO ethane barrier, and we find a simple explanation which holds for both the geometry-optimized and frozen-frame barriers. Emphasized are the effects of geometry optimization on the various energy terms, and comparisons between INDO and *ab initio* calculations are given whenever possible.

I. General Theory

Consider a molecule which has N occupied molecular orbitals and M atoms. If Z_A is the atomic number of atom A and λ_i is the ith energy-localized molecular orbital, one can often assign localized positive distributions to the λ_i's in the following manner

$$\begin{aligned} Z_i(\mathrm{A}) &= 2 \text{ if } \lambda_i \text{ is a lone-pair (lp) or inner-shell (is) orbital localized on atom A} \\ &= 1 \text{ if } \lambda_i \text{ is a bond orbital (bo) localized on atom A} \\ &= 0 \text{ otherwise} \end{aligned} \quad (1)$$

where $Z_i(\mathrm{A})$ is that part of the positive charge on atom A assigned to λ_i and

$$\sum_i Z_i(\mathrm{A}) = Z_\mathrm{A} \quad (2)$$

While the types of localized orbitals described in (1) are those most frequently encountered, other cases do arise and may be dealt with straightforwardly, *e.g.*, for BF where, in addition to one (inner shell) and one lone-pair orbital on each nucleus, there occur three bond orbitals between B and F;[18] the nuclear partitioning would be $Z_{is}(\mathrm{B}) = 2$, $Z_{lp}(\mathrm{B}) = 2$, $Z_{bo}(\mathrm{B}) = {}^1/_3$, $Z_{is}(\mathrm{F}) = 2$, $Z_{lp}(\mathrm{F}) = 2$, $Z_{bo}(\mathrm{F}) = {}^5/_3$. Once the $Z_i(\mathrm{A})$'s are defined, it is possible to partition any molecular expectation value of interest into localized contributions.

(1) Work was performed in the Ames Laboratory of the U. S. Atomic Energy Commission, Contribution No. 2870.
(2) C. Edmiston and K. Ruedenberg, *Rev. Mod. Phys.*, **35**, 457 (1963).
(3) C. C. J. Roothaan, *ibid.*, **23**, 69 (1951).
(4) J. A. Pople, D. L. Beveridge, and P. A. Dobosh, *J. Chem. Phys.*, **47**, 2026 (1967).
(5) K. Ruedenberg, *Rev. Mod. Phys.*, **34**, 326 (1962).
(6) I. R. Epstein and W. N. Lipscomb, *J. Amer. Chem. Soc.*, **92**, 6094 (1970).
(7) M. S. Gordon, *ibid.*, **91**, 3122 (1969).
(8) O. Sovers and M. Karplus, *J. Chem. Phys.*, **44**, 3033 (1966).
(9) A. Veillard, *Chem. Phys. Lett.*, **3**, 128 (1969).
(10) W. L. Clinton, *J. Chem. Phys.*, **33**, 632 (1960).
(11) M. Karplus and R. G. Parr, *ibid.*, **38**, 1547 (1963).
(12) J. P. Lowe, *ibid.*, **45**, 3055 (1966).
(13) E. Clementi and D. R. Davis, *ibid.*, **45**, 2593 (1966).
(14) W. H. Fink and L. C. Allen, *ibid.*, **46**, 2262 (1967).
(15) R. M. Pitzer, *ibid.*, **41**, 2216 (1964).
(16) K. Ruedenberg, *ibid.*, **41**, 588 (1964).
(17) J. A. Pople and G. A. Segal, *ibid.*, **43**, S136 (1965).
(18) C. Edmiston and K. Ruedenberg, *ibid.*, **43**, S97 (1965).

The total energy, E, for example, may be written as

$$E = \sum_{i=1}^{N} e_i \tag{3}$$

within the Born–Oppenheimer approximation, where

$$e_i = \tau_i + \sum_{j=1}^{N} v_{ij} \tag{4}$$

is the total energy of the ith distribution (λ_i plus $Z_i(\mathrm{A})$ for all atoms A)

$$\tau_i = N_i \int \mathrm{d}V_1 \lambda_i(1)[-{}^1/_2\nabla_1{}^2]\lambda_i(1) \tag{5}$$

is the kinetic energy of the ith distribution in atomic units

$$v_{ij} = V_{ij} + G_{ij} + g_{ij} \tag{6}$$

is the potential energy of interaction between distributions i and j, and v_{ii} and v_{ij} are the intra- and interdistribution contributions, respectively, to the total potential energy of distribution i. The terms on the right-hand side of eq 6 are

$$V_{ij} = -{}^1/_2 \int \mathrm{d}V_1 \sum_{\mathrm{A}=1}^{M} [\rho_i(1, 1)Z_j(\mathrm{A}) + \rho_j(1, 1)Z_i(\mathrm{A})](1/R_{\mathrm{A}1}) \tag{7}$$

$$G_{ij} = {}^1/_2 \int \mathrm{d}V_1 \int \mathrm{d}V_2 (1/r_{12})[\rho_i(1, 1) \times \rho_j(2, 2) - {}^1/_2\rho_i(1, 2)\rho_j(1, 2)] \tag{8}$$

$$g_{ij} = {}^1/_2 \sum_{\mathrm{A}=1}^{M} \sum_{\mathrm{B}\neq\mathrm{A}} \frac{Z_i(\mathrm{A})Z_j(\mathrm{B})}{R_{\mathrm{AB}}} \tag{9}$$

$R_{\mathrm{A}1}$ is the distance between atom A and electron 1, r_{12} is the distance between electrons 1 and 2, R_{AB} is the internuclear distance, and

$$\rho_i(1, 2) = N_i \lambda_i(1)\lambda_i(2) \tag{10}$$

with N_i = the occupation number of λ_i, is the electron density of λ_i. Equations 7, 8, and 9 represent the attractive electrostatic energy, electron repulsion energy, and nuclear repulsion energy, respectively, between distributions i and j.

II. Approximate Localized Orbitals

When approximate localized orbitals are used, it may no longer be possible to obtain the general inter- and intradistribution partitioning. An example is furnished by the INDO valence-orbital approximation[4] employed later in this work.

As in all valence-orbital theory, the core charges

$$\begin{aligned} Q_{\mathrm{A}} &= Z_{\mathrm{A}} - 2 \text{ if A is not hydrogen} \\ &= Z_{\mathrm{A}} \text{ if A is hydrogen} \end{aligned} \tag{11}$$

replace the Z_{A} and thereby the normalization condition in (2) becomes

$$\sum_{i=1}^{N} Q_i(\mathrm{A}) = Q_{\mathrm{A}} \tag{12}$$

with N now the number of valence orbitals.

Each localized valence orbital has the form

$$\lambda_i = \sum_{\mu} \chi_\mu C_\mu{}^i : \sum_{\mu} C_\mu{}^i C_\mu{}^j = \delta_{ij} \tag{13}$$

where χ_μ is a Slater-type orbital (STO), $C_\mu{}^i$ is an LCAO expansion coefficient, and δ_{ij} is the Kronecker delta. In the INDO approximation, (4) is written as

$$e_i = \sum_{\mathrm{A}=1}^{M} U_i(\mathrm{A}) + \sum_{\mathrm{A}=1}^{M} \sum_{\mathrm{B}\neq\mathrm{A}} \left\{ \beta_i(\mathrm{A}, \mathrm{B}) + \sum_{j=1}^{N} V_{ij}(\mathrm{A}, \mathrm{B}) \right\} + \sum_{j=1}^{N} (G_{ij} + g_{ij}) \tag{14}$$

where

$$U_i(\mathrm{A}) = \sum_{\mu} (C_\mu{}^i)^2 \int \mathrm{d}V_1 \chi_\mu(1)[-{}^1/_2\nabla_1{}^2 - \sum_j Q_j(\mathrm{A})/R_{\mathrm{A}1}]\chi_\mu(1) = \sum_{\mu} (C_\mu{}^i)^2 U_{\mu\mu} \tag{15}$$

$$\beta_i(\mathrm{A}, \mathrm{B}) = \sum_{\mu}^{\mathrm{A}} \sum_{\nu}^{\mathrm{B}} C_\mu{}^i C_\mu{}^j \int \mathrm{d}V_1 \chi_\mu(1) \left\{ -{}^1/_2\nabla_1{}^2 - \sum_{j=1}^{N} [Q_j(\mathrm{A})/R_{\mathrm{A}1} + Q_j(\mathrm{B})/R_{\mathrm{B}1}] \right\} \chi_\nu(1) = \sum_{\mu}^{\mathrm{A}} \sum_{\nu}^{\mathrm{B}} C_\mu{}^i C_\nu{}^j \beta_{\mu\nu} \tag{16}$$

and

$$V_{ij}(\mathrm{A}, \mathrm{B}) = -\sum_{\mu}^{\mathrm{A}} \int \mathrm{d}V_1 \chi_\mu{}^2(1)/R_{\mathrm{B}1}[(C_\mu{}^i)^2 Q_j(\mathrm{B}) + (C_\mu{}^j)^2 Q_i(\mathrm{B})] \tag{17}$$

The subscript A on a summation means that the sum is to be taken over all basis orbitals on atom A.

Since the matrix elements $U_{\mu\mu}$ and $\beta_{\mu\nu}$ are explicitly parametrized, the partitioning employed in (5)–(7) is unworkable. The parametrization does not affect, however, the partitions given by (8)–(17). The remaining energy terms, $V_{ij}(\mathrm{A}, \mathrm{B})$, G_{ij}, and g_{ij} are obtained directly from the corresponding INDO expressions.[4]

III. Interpretation of the INDO Partition

The quantities G_{ij} and g_{ij} admit the same interpretation previously given and will not be discussed further. In order to interpret the one-electron terms, we shall use the description of bonding originated by Ruedenberg.[5] This description employs quasiclassical densities which, in analogy with the densities of classical electrostatics, may be superposed to form new densities and interference densities which occur in any wave theory and represent an enhancement (constructive interference) or attenuation (destructive interference) of phase. In quantum mechanics the waves are matter waves, and interference corresponds to build-up or depletion of matter (which at present may be conveniently discussed as an accumulation or depletion of negative charge). Ruedenberg developed these ideas for both the density and pair density of general antisymmetric wave functions,[5] but we shall herein be concerned only with the density partitioning.

Application of Ruedenberg's distribution partitioning[5] to our orbital densities gives

$$\rho_i(1, 2) = \rho_i{}^{\mathrm{Cl}}(1, 2) + \rho_i{}^{\mathrm{I}}(1, 2) \tag{18}$$

where

$$\rho_i{}^{\mathrm{Cl}}(1, 2) = N_i \sum_{\mathrm{A}=1}^{M} \sum_{\mu}^{\mathrm{A}} \sum_{\nu}^{\mathrm{A}} C_\mu{}^i C_\nu{}^i \chi_\mu(1)\chi_\nu(2) \tag{19}$$

is the quasiclassical orbital density, and

$$\rho_i{}^{\mathrm{I}}(1, 2) = N_i \sum_{\mathrm{A}=1}^{M} \sum_{\mathrm{B}\neq\mathrm{A}} \sum_{\mu}^{\mathrm{A}} \sum_{\nu}^{\mathrm{B}} C_\mu{}^i C_\nu{}^i \chi_\mu(1)\chi_\nu(2) \tag{20}$$

Table I. Geometries and Relative Energies[a] in Ethane Isomers

	R_{CC}, Å	R_{CH}, Å	∠HCC, deg	∠HCH, deg		Nuclear repulsion	Electron repulsion	Barrier
Staggered OPT	1.46	1.12	112.2	106.6	OPT	−7.85	−8.48	2.25
Eclipsed OPT	1.46	1.12	112.7	106.1	MBLD	4.68	4.74	2.20
Staggered MBLD	1.54	1.09	109.5	109.5	Exptl[b]			2.875
Eclipsed MBLD	1.54	1.09	109.5	109.5				
Exptl[b]	1.536	1.108	110.1	108.8				

[a] Energies are in kilocalories per mole. [b] W. J. Lafferty and E. K. Plyler, *J. Chem. Phys.*, **37**, 2688 (1962).

is the orbital interference density. It should be noted that the quasiclassical density is a superposition of atomic contributions, whereas the interference density is due only to diatomic terms and is short range in character; *i.e.*, the atoms involved must interfere, or overlap. (N.B. Even orthogonal functions may overlap; only their inner product vanishes.) Moreover, even though the INDO interference and overlap distributions are identical (owing to the neglect of differential overlap) $\rho_i^I(1, 2)$ *is not to be generally interpreted as an overlap distribution.* This is discussed in detail by Ruedenberg.[5]

The one-electron quasiclassical INDO energy consists of two parts, the one-center energies

$$U_i = \sum_{A=1}^{M} U_i(A) \tag{21}$$

and the two-center electron–nucleus attraction energy

$$V_{ij} = \sum_{A=1}^{M} \sum_{B \neq A} V_{ij}(A, B) \tag{22}$$

which may be either inter ($i \neq j$) or intra ($i = j$) in character. Equations 21 and 22 follow straightforwardly from the results of the preceding paragraph and the INDO parameterization. Similarly, the one-electron interference energy for the ith localized distribution is

$$\beta_i = \sum_{A=1}^{M} \sum_{B \neq A} \beta_i(A, B) \tag{23}$$

and, as such, it is the prototype of those terms "... which represent the primordial source for the positive or negative stabilization energy which leads to chemical binding and antibinding."[5]

IV. Analysis of Energy Barrier in Ethane

Preliminary. Two calculations were undertaken for ethane, one in which the geometry was obtained by energy optimization (OPT) and one in which the geometry was assigned using the model builder (MBLD) described previously.[19,20] The numbering of the atoms is the same in each case and is given in Figure 1. Geometries, barriers, and repulsion energy differences are shown in Table I. (Throughout this work, we obtain energy differences by subtracting the energy term for staggered ethane from the corresponding term for eclipsed ethane.)

It is found in the OPT calculation that, in passing from the staggered to the eclipsed isomers, the only geometry changes apart from the dihedral angle are increases of 0.5° in the HCC angles (and decreases of 0.5° in the HCH angles). Both calculations account for about 75% of the experimental barrier and predict that the barrier due to nuclear repulsion is similar to that due to electron repulsion. A striking difference, however, is provided by the fact that in the OPT calculation both repulsion barriers (electron and nuclear) favor the eclipsed rotamer, whereas the MBLD repulsion barriers favor the staggered rotamer. Thus, geometry optimization, while leaving the total barrier virtually unchanged, has introduced a fundamental difference within that part of the barrier due to repulsive interactions. The former result has been known to obtain within the CNDO/2 theory[21] and Stevens[22] and Epstein and Lipscomb[6] have recently demonstrated it in the *ab initio* case. The latter authors, using Stevens'[22] results, have also pointed out that the various energy components of the barrier are strongly affected by geometry optimization. In particular, they found that the nuclear repulsion barrier favors the eclipsed isomer by about 70 kcal/mol, or ten times our result. The fundamental nature of this difference follows from the results of Clinton[10] who, using the virial theorem for polyatomic molecules, was able to show quite simply that for an internal rotation the equalities, total barrier = ½ potential barrier = −kinetic barrier, must hold. He then showed that in ethane—without geometry optimization—the total barrier is closely one-half the nuclear repulsion barrier, and thereby remaining potential energy contributions to the barrier cancel. Our results, and also those of Stevens,[22] suggest that this last fact is no longer true when the geometry is optimized. We contend, therefore, that *any interpretation of the ethane barrier which assumes that the nuclear repulsion energy is lower in the staggered form is likely to be unrealistic.* This does not imply, however, that calculations on ethane undergoing frozen-frame rotation *necessarily* give unrealistic explanations of the barrier, as we shall see below.

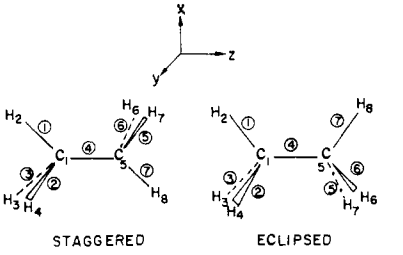

Figure 1. Choice of coordinate system and numbering of atoms and bonds in ethane.

(19) J. A. Pople and M. Gordon, *J. Amer. Chem. Soc.*, **89**, 4253 (1967).
(20) M. Gordon and J. A. Pople, Quantum Chemistry Program Exchange, Program No. 135.
(21) J. A. Pople and G. A. Segal, *J. Chem. Phys.*, **44**, 3289 (1966).
(22) R. M. Stevens, *ibid.*, **52**, 1397 (1970).

Table II. Localized Orbitals in Ethane[a]

Atomic orbitals	Staggered OPT 1	Staggered OPT 4	Eclipsed OPT 1	Eclipsed OPT 4	Staggered MBLD 1	Staggered MBLD 4	Eclipsed MBLD 1	Eclipsed MBLD 4
$C_1(2s)$	0.3484	0.3927	0.3476	0.3949	0.3577	0.3691	0.3577	0.3692
$C_1(2p_x)$	0.5563	0.0000	0.5568	0.0000	0.5588	0.0000	0.5591	0.0000
$C_1(2p_y)$	0.0000	0.0000	0.0000	0.0000	0.0000	0.0000	0.0000	0.0000
$C_1(2p_z)$	−0.2306	0.5880	−0.2309	0.5865	−0.2190	0.6031	−0.2190	0.6031
H_2	0.7128	−0.0046	0.7128	−0.0054	0.7115	−0.0005	0.7115	−0.0006
H_3	−0.0115	−0.0046	−0.0110	−0.0054	−0.0123	−0.0005	−0.0123	−0.0006
H_4	−0.0115	−0.0046	−0.0110	−0.0054	−0.0123	−0.0005	−0.0123	−0.0006
$C_5(2s)$	−0.0053	0.3927	−0.0055	0.3949	−0.0055	0.3691	−0.0057	0.3692
$C_5(2p_x)$	0.0632	0.0000	0.0624	0.0000	0.0518	0.0000	0.0505	0.0000
$C_5(2p_y)$	0.0000	0.0000	0.0000	0.0000	0.0000	0.0000	0.0000	0.0000
$C_5(2p_z)$	−0.0070	−0.5880	−0.0071	−0.5865	−0.0041	−0.6031	−0.0042	−0.6031
H_6	−0.0193	−0.0046	0.0291	−0.0054	−0.0158	−0.0005	0.0238	−0.0006
H_7	−0.0193	−0.0046	0.0291	−0.0054	−0.0158	−0.0005	0.0238	−0.0006
H_8	0.0535	−0.0046	−0.0429	−0.0054	0.0441	−0.0005	−0.0347	−0.0006

[a] Units are $(\text{bohr})^{-3/2}$.

Table III. Repulsive and Quasiclassical Attractive Electrostatic Bond Interactions[a]

	Orbital, i = 1	2	3	4	5	6	7	Total
				OPT				
ΔV_{1i}	−1.3	−8.9	−8.9	7.0	308.3	308.3	−569.0	35.5
ΔG_{1i}	1.5	5.7	5.7	−3.7	−153.2	−153.2	278.1	−19.1
Δg_{1i}	0.0	5.3	5.3	−3.5	−151.4	−151.4	278.3	−17.4
ΔR_{1i}	0.2	2.1	2.1	−0.2	3.7	3.7	−12.6	−1.0
ΔV_{4i}	7.0	7.0	7.0	−0.3	7.0	7.0	7.0	41.7
ΔG_{4i}	−3.7	−3.7	−3.7	1.5	−3.7	−3.7	−3.7	−20.7
Δg_{4i}	−3.5	−3.5	−3.5	0.0	−3.5	−3.5	−3.5	−21.0
ΔR_{4i}	−0.2	−0.2	−0.2	1.2	−0.2	−0.2	−0.2	0.0
				MBLD				
ΔV_{1i}	−1.0	1.1	1.1	0.4	294.2	294.2	−613.0	−23.0
ΔG_{1i}	2.0	1.6	1.6	0.2	−147.3	−147.3	301.4	12.2
Δg_{1i}	0.0	0.0	0.0	0.0	−145.1	−145.1	302.6	12.4
ΔR_{1i}	1.0	2.7	2.7	0.6	1.8	1.8	−9.0	1.6
ΔV_{4i}	0.4	0.4	0.4	0.0	0.4	0.4	0.4	2.4
ΔG_{4i}	0.2	0.2	0.2	0.1	0.2	0.2	0.2	1.1
Δg_{4i}	0.0	0.0	0.0	0.0	0.0	0.0	0.0	0.0
ΔR_{4i}	0.6	0.6	0.6	0.1	0.6	0.6	0.6	3.5
				Ab Initio[b]				
ΔG_{1i}	5.6	6.3	6.3	0.2	−180.9	−180.9	360.9	17.2
ΔG_{4i}	0.2	0.2	0.2	0.5	0.2	0.2	0.2	1.7

[a] Units are au $\times 10^{-4}$. [b] R. M. Pitzer, *J. Chem. Phys.*, **41**, 2216 (1964).

The question naturally arises: How realistic are our optimized semiempirical geometries? Stevens' geometries,[22] which are closer to the experimental results, predict that accompanying the rotation from staggered to eclipsed are a decrease of 0.002 Å in the R_{CH} and increases of 0.016 Å and 0.3°, respectively, in the CC bond length and CCH angle. His barrier is 3.3 kcal/mol. Thus, even though our bond lengths are clearly too short, our angular distortion and the magnitude of the deviation of our barrier from experiment are quite similar to the values from the *ab initio* calculation. For this reason, we assume that a realistic barrier interpretation may be given with the INDO results.

Energy localization with the Edmiston–Ruedenberg method[2] yields for both rotational isomers one CC bond orbital and six equivalent CH bond orbitals. These appear in Table II, and it follows that the localized distributions of positive charge can be obtained from (1). Each neutral distribution is referred to as a bond. Note that only one CH orbital is presented for each case, the others being defined by symmetry. We have shown elsewhere that INDO-localized orbitals are in good agreement with existing *ab initio* localized orbitals.[23]

Bonds are numbered the same way in both calculations and appropriate spatial locations relative to the given orbitals may be determined using Figure 1. For example, bond 7 is the CH bond trans (cis) to bond 1 in the staggered (eclipsed) rotamer.

Repulsive and Quasiclassical Two-Center Attractive Bond Interactions. CH Bonds. The net changes in the repulsion energies of the CH bond, Δg_1 and ΔG_1, which appear in the last column of Table III, follow the same trend as the total repulsion energies; *i.e.*, g_1 and G_1 are smaller for the eclipsed isomer in the OPT calculation and smaller for the staggered isomer in the MBLD calculation. The corresponding quasiclassical two-center attractions, V_1, display exactly opposite trends. This disparity between the OPT and MBLD results can be understood by examining the inter- and intrabond partitioning given in Table III.

(23) W. England and M. S. Gordon, *J. Amer. Chem. Soc.*, **91**, 6864 (1969).

Table IV. One-Electron One-Center Energies[a]

	Core A = 1	2	3	4	5	6	7	8	Total
				OPT					
ΔU_1(A)	−2.6	−0.6	0.1	0.1	4.1	−6.1	−6.1	13.1	2.0
ΔU_4(A)	−9.8	−0.1	−0.1	−0.1	−9.8	−0.1	−0.1	−0.1	−20.2
				MBLD					
ΔU_1(A)	−10.8	0.1	0.0	0.0	5.5	−4.0	−4.0	9.5	−3.7
ΔU_4(A)	−0.5	0.0	0.0	0.0	−0.5	0.0	0.0	0.0	−1.0

[a] Units are au × 10^{-4}.

In both calculations changes in V_{1i}, g_{1i}, and G_{1i} involving the same bond (i = 1) or nearest-neighbor bonds (i = 2, 3, 4) are two orders of magnitude smaller than those between the vicinal bonds (i = 5, 6, 7), which are rotated relative to one another. Among the latter, it can be seen that differences between the OPT and MBLD interactions for the gauche bonds (i = 5, 6) are lower in magnitude than those for the coplanar bonds (i = 7, cis or trans) by about a factor of 3. In fact, the opposite trends observed in the quantities ΔV_1, ΔG_1, and Δg_1 are seen to be primarily covered by the differences between the OPT and MBLD coplanar bond interactions (*i.e.*, the interaction between bonds 1 and 7). It is important to note, however, that total changes in the electrostatic energy

$$\Delta R_{1i} = \Delta V_{1i} + \Delta G_{1i} + \Delta g_{1i} \qquad (24)$$

closely follow the same pattern in both calculations. Thus, the overall effect of the geometry optimization on the ΔR_{1i} is far different from its effect on the quantities ΔV_{1i}, ΔG_{1i}, and Δg_{1i} separately. The similarity of the ΔR_{1i}(OPT) and ΔR_{1i}(MBLD) values, coupled with the opposite behavior of the individual terms, shows that the magnitudes of ΔV_{1i}, ΔG_{1i}, and Δg_{1i} all change in nearly the same ratio in going from the OPT to the MBLD calculation. This result can be understood by considering the approximate equalities

$$\Delta G_{1i} \approx \Delta g_{1i} \approx -{}^1/_2 \Delta V_{1i} \qquad (25)$$

which are observed in both calculations. The first relation ($\Delta G_{1i} \approx \Delta g_{1i}$) shows that, with regard to changes in repulsion, the positive and negative charge distributions of each bond behave in essentially the same way, while the second equality shows that changes in the quasiclassical two-center attractions between the positive and negative charges of bond pairs oppose and almost cancel these repulsions. Thus, *certain* results which are rigorously true for rigid bond distributions (those whose shape and volume are unchanged) which do not overlap obtain to a good approximation within the real molecule. These electrostatic changes, therefore, give the appearance that the electrons are localized near the cores of the bond and, furthermore, repulsions among electrons localized near the same core (*i.e.*, two adjacent bonds) are almost independent of the conformation. It should be well noted that the quasiclassical electrostatic one-center terms (those in U_i(A)) have not been included in this discussion, nor have the interference electrostatic attractions (those in β_i(A, B)). Finally, we feel that the first approximate equality (25) gives special credence to our partitioning of the positive charge distribution.

CC Bonds. All electrostatic quantities V_{4i}, G_{4i}, and g_{4i} are virtually independent of the conformation in the MBLD calculation, but ΔV_{4i}, ΔG_{4i}, and Δg_{4i} in the OPT calculation are all seen to change. Upon rotation from staggered to eclipsed ethane, the repulsive interactions decrease and the attractive interactions increase, in keeping with the fact that the C–nonbonded H bond lengths are slightly longer in the eclipsed isomer, whereas both the C–C and the C–bonded H bond lengths are unchanged. Since approximate relations similar to (25) are also satisfied here, a parallel analysis can be used to show that changes in either the OPT or MBLD ΔV_{4i}, Δg_{4i}, and ΔG_{4i} values can be considered to arise from electrons localized near the cores, and interactions involving pairs of electrons localized near the same centers are the same in both isomers. Furthermore, it follows from

$$\begin{aligned} \Delta V_4(\text{OPT}) &\approx \Delta V_1(\text{OPT}) \\ \Delta G_4(\text{OPT}) &\approx \Delta G_1(\text{OPT}) \\ \Delta g_4(\text{OPT}) &\approx \Delta g_1(\text{OPT}) \end{aligned} \qquad (26)$$

that the OPT CC bond contributes almost as much to the *total* changes observed in the repulsion energies and the quasiclassical two-center attraction energy as does an OPT CH bond.

Comparison of MBLD and *Ab Initio* Repulsions. The *ab initio* localized *valence*-orbital electron repulsions reported by Pitzer[15] are reproduced in the last two rows of Table III. Since his geometry[24] is very close to the MBLD geometry, the Δg_{1i} values can be considered the same as those for MBLD. His barrier is 3.3 kcal/mol.

There is only fair agreement between the MBLD and Pitzer ΔG_{1j} values, but the ΔG_{4j} values are almost identical. The *ab initio* ΔG_1 is due to changes in the repulsions between geminal CH bonds, while the MBLD ΔG_1 is only about 50% due to such repulsions, the remainder being due to repulsions from the vicinal CH orbitals.

The most striking difference between the two calculations is that the approximate relation $\Delta G_{ij} \approx \Delta g_{ij}$ does not hold for the *ab initio* CH orbitals. In view of the discussion previously given, it may be that in INDO repulsion integrals approximate such that the electrons are associated too closely with the cores; *i.e.*, the short-range repulsions are underemphasized. The more pertinent comparison of our OPT results with those for an *ab initio* geometry-optimized calculation is not presently possible.

One-Electron One-Center Energies. CH Bonds. The one-center contributions to the OPT and MBLD CH bonds (Table IV) are very similar except on the bonded

(24) R. M. Pitzer and W. N. Lipscomb, *J. Chem. Phys.*, **39**, 1995 (1963).

Table V. One-Electron Interference Energies[a]

	OPT	MBLD		OPT	MBLD
$\Delta\beta_1$(1, bonded H's)	0.2	−1.6	$\Delta\beta_1$(5, nonbonded H's)	2.2	1.5
$\Delta\beta_1$(1, 5)	2.9	4.2	$\Delta\beta_1$(6, 7) + $2\Delta\beta_1$(6, 8)	0.0	−0.1
$\Delta\beta_1$(1, nonbonded H's)	−1.6	−1.3	$\Delta\beta_1$	7.8	7.3
$\Delta\beta_1$(2, geminal H's)	−1.2	0.0	$2\Delta\beta_4$(C, bonded H's)	9.1	1.1
$\Delta\beta_1$(2, vicinal H's)	6.5	5.9	$\Delta\beta_4$(1, 5)	−19.5	−1.0
$\Delta\beta_1$(3, 4)	0.0	0.0	$2\Delta\beta_4$(C, nonbonded H's)	12.4	1.2
$2\Delta\beta_1$(3, vicinal H's)	0.0	0.1	$\Delta\beta_4$(geminal H's)	−0.1	0.0
$\Delta\beta_1$(5, bonded H's)	−1.2	−1.4	$\Delta\beta_4$(vicinal H's)	−0.1	0.0
			$\Delta\beta_4$	1.8	1.3

[a] Energies in au × 10^{-4}.

carbon (C_1). Since

$$\sum_{A=2}^{8} \Delta U_1(A) = 4.6 \times 10^{-4} \text{ au (OPT)}$$

and

$$\sum_{A=2}^{8} \Delta U_1(A) = 7.1 \times 10^{-4} \text{ au (MBLD)}$$

it is apparent that the difference in ΔU_1(OPT) and ΔU_1(MBLD) arises from the difference in $\Delta U_1(1)$ for the two calculations. Changes in $U_i(A)$ may be due either to changes in hybridization (per cent s character) and/or to changes in the net electron density on atom A due to orbital i ($P_i(A)$). Since

$$\Delta P_1^{OPT}(1) \approx \Delta P_1^{MBLD}(1) \approx -0.0004$$

and since there is virtually no difference in the CH orbital between MBLD eclipsed and staggered ethane, one can conclude that the change in $U_1(1)$ due to density changes ≈ -0.0011 au in both calculations. Since $\Delta U_1^{OPT}(1) \approx -0.0003$ au, it becomes clear that the difference between the $\Delta U_1(1)$'s, and hence the difference between the ΔU_1's themselves, is due to the fact that the OPT CH orbital is of slightly increased 2s character in the staggered isomer. This follows from the fact that $U_{2s,2s} < U_{2p,2p}$. Another interesting point is that in both calculations the contribution of the trans (or cis) hydrogen (8) is effectively canceled by the two gauche hydrogens (6 and 7), and similarly

$$\Delta P_1(6) + \Delta P_1(7) + \Delta P_1(8) \approx 0$$

CC Bonds. Here, too, a difference between the two calculations arises because of differing contributions from bond carbons since, apart from the increases on the carbon cores in the OPT case, all one-center contributions are independent of conformation. For the CC bonds

$$\Delta P_4^{OPT}(1) \approx 0.0002$$

so here the density change favors the staggered rotamer. Since $\Delta U_4^{OPT}(1)$ favors the eclipsed conformation, $\Delta U_4^{OPT}(1)$, and hence ΔU_4^{OPT} itself, is due to the increased 2s character in the eclipsed form.

The 2s character can be related to distortions in the HCC and HCH angles by considering hybrids on the carbon atoms. Let

$$t_z = \cos \alpha(2s) + \sin \alpha(2p_z) \quad (27)$$

represent the hybrid pointing toward the other carbon and let

$$t_i = \cos \beta(2s) + \sin \beta(2p_i) \quad (28)$$

be one of three equivalent hybrids which point approximately toward the hydrogens. The functions $2p_i$ are linear combinations of the $2p_x$, $2p_y$, and $2p_z$ orbitals, with $\alpha = \beta = 60°$ for pure sp^3 hybrids. We require these hybrids to be mutually orthogonal

$$\int t_i(1)t_z(1)dV_1 = \cos \alpha \cos \beta + \sin \alpha \sin \beta \cos \theta = 0 \quad (29)$$

where θ is the angle between hybrids t_i and t_z. Similarly, for two CH hybrids t_i and t_j

$$\int t_i(1)t_j(1)dV_1 = \cos^2 \beta + \sin^2 \beta \cos \phi = 0 \quad (30)$$

ϕ being the angle between hybrids t_i and t_j. Equation 29 gives

$$\tan \alpha \tan \beta = -1/\cos \theta \quad (31)$$

while (30) results in

$$\tan \beta = 1/(-\cos \phi)^{1/2} \quad (32)$$

Recalling that a small decrease in the HCH angle occurs upon rotation from staggered to eclipsed, one finds a decrease in $-\cos \phi$ if the hybrids at least partially follow the compression. This corresponds to a decrease in $\cos \beta$. Assuming the hybrid t_z remains pointed toward the other carbon and since both $\tan \beta$ and the HCC angle increase, one finds that $\cos \alpha$ increases. Finally, if this reasoning may be directly carried over to the case of localized orbitals, the 2s character of the CC orbital should increase and the 2s character of the CH orbital should decrease upon rotation from staggered to eclipsed. This is, indeed, just what we observe, and therefore we attribute it to the angular distortions.

One-Electron Interference Energies. Table V contains the one-electron interference energy differences, $\Delta\beta_i$(A, B), for CH and CC orbitals obtained in both the OPT and MBLD calculations. For each localized orbital, the interference terms are grouped according to particular types of atom pairs. For example, the interactions between core 2 and its geminal hydrogens 3 and 4 (see Figure 1) comprise one grouping referred to as $\Delta\beta_i$(2, geminal H's), while the interactions between carbon 1 and its bonded hydrogens sum to give $\Delta\beta_i$(1, bonded H's). In this spirit each group consists of interactions between cores or groups of cores which are either neighbors, next neighbors, or next to next neighbors; *i.e.*, the interactions are grouped according to range order.

CH Bonds. Within a particular group, the energy changes quoted for the OPT calculation are seen to be

quite similar to those for the MBLD calculation; thus the groups of CH bond energy differences are not greatly affected by geometry optimization. As can be seen from Table V, in both calculations $\Delta\beta_1$ is primarily due to changes in the interference energy between the bonded hydrogen and those hydrogens vicinal to it. Specifically, as can be verified by comparing the appropriate coefficients in Table II, it is found that in the staggered conformation there is constructive interference, or covalent binding ($\beta_1(2, 8)$ is negative), between the bond and trans hydrogens and destructive interference, or anticovalent binding ($\beta_1(2, 6)$ is positive), between the bond hydrogen and each of the two gauche hydrogens. In the eclipsed conformation, on the other hand, there is destructive interference between the bond and cis hydrogens and constructive interference between the bond hydrogen and each of its gauche hydrogens. Thus, in either calculation and in both isomers, it emerges that within a given CH orbital there is interference antibinding between the bond hydrogen and the vicinal hydrogen(s) nearest it and interference binding between the bond hydrogen and the vicinal hydrogen(s) farthest from it. Furthermore, from the relations

$$\Delta\beta_1(2, 8) = 43.2 \quad \text{(OPT)}$$

$$\Delta\beta_1(2, 6) + \Delta\beta_1(2, 7) = -36.7 \quad \text{(OPT)}$$

and

$$\Delta\beta_1(2, 8) = 38.2 \quad \text{(MBLD)}$$

$$\Delta\beta_1(2, 6) + \Delta\beta_1(2, 7) = -32.2 \quad \text{(MBLD)}$$

the preference for the staggered isomer is seen to be due to the change from constructive to destructive interference between that portion of the orbital localized near the bond hydrogen and the "tail" or overflow portion of the orbital near the coplanar hydrogen. As will be seen later, this result is very important in connection with the total barrier. A final point worth noticing is that, unlike the behavior discussed in previous sections, the present findings necessarily owe their existence to the fact that the localized orbitals are not totally confined to two centers; *i.e.*, these results are due to a generalized "hyperconjugation" in which there is a significant overflow of charge density from a σ bond to nonbonded vicinal atoms. This same behavior has been observed for paraffins in localized bond studies by Pople and Santry,[25] who stressed its importance with regard to vicinal interactions and stated its correspondence to the "second order hyperconjugation" discussed by Mulliken, *et al.*[26] Peters[27] noticed this same behavior in yet another context and termed it "sigma-conjugation."

CC Bonds. The total change in the interference energy of the CC bond, $\Delta\beta_4$, is seen to be small in both calculations, but for different reasons. All contributions in the MBLD case are small, while in the OPT case this is true only of changes in the hydrogen–hydrogen interferences. The effect of the changed HCC angle on the OPT CC orbital is to increase the magnitude both of the constructive interference between the two carbons and the destructive interferences among the carbon and hydrogens relative to the staggered conformation, but in such a way that the net effect is small. Therefore, the geometry optimization affects the CC bond interference only in a "local" manner, there being no net change because of a cancellation which involves groups of different range interactions.

Bond Energy Analysis of the Barrier. Table VI lists energy changes already analyzed, but with slight differences due to round off in previous tables. The last column lists the total bond energy changes, which are defined as

$$\Delta e_i = \Delta U_i + \Delta\beta_i + \Delta R_i \qquad (33)$$

in keeping with (14).

Table VI. Bond Energy Contributions[a]

Orbital	ΔU_i	$\Delta\beta_i$	ΔR_i	Δe_i
		OPT		
1	2.0	7.9	−1.0	8.9
4	−20.3	1.9	0.0	−18.4
		MBLD		
1	−3.7	7.2	1.6	5.1
4	−1.1	1.4	3.5	3.8

[a] Units are au × 10^{-4}.

OPT Calculation. There is opposition between the CC and CH bonds, the total energy of the CH bond favoring the staggered conformation largely because of the $\Delta\beta_1$ term, and the total energy of the CC bond favoring the eclipsed rotamer because of the ΔU_4 term. Moreover, the CC bond changes by a magnitude twice that of the CH bonds: the deciding factor, then, is not that the CC bond is unchanged, but rather that there are six CH bonds involved. *The interpretation of the barrier is that the CC bond favors the eclipsed rotamer due to its slightly increased 2s character, while the CH bonds favor the staggered conformation because of the increased constructive interference between electrons localized near the bond and coplanar hydrogens. The interference change, though smaller in magnitude, dominates because it occurs in each CH bond.*

MBLD Calculation. Upon internal rotation, the MBLD CC bond changes much less than in the OPT case. This agrees with Pitzer's results[15] and is usually assumed when interpreting the ethane barrier. Furthermore, Δe_4 parallels the change in the CH bonds. This is fundamentally different from the OPT results, where the CC bond was found to strongly favor the eclipsed rotamer. Therefore, *the MBLD barrier is due almost entirely to the CH bonds and these bonds favor the staggered isomer for the same reason as in the OPT calculation.*

Interference Energy Analysis of the Barrier. The present discussion rests on the substantial energy changes predicted by both calculations due to the differing interferences in the CH bonds between the bond hydrogens and those vicinal to them. These effects were shown to favor the staggered conformation and, in particular

$6\Delta\beta_1(2, \text{vicinal H's}) =$
39×10^{-4} au $\approx 109\%$ of barrier (OPT)

$6\Delta\beta_1(2, \text{vicinal H's}) =$
35.4×10^{-4} au $\approx 101\%$ of barrier (MBLD)

(25) J. A. Pople and D. P. Santry, *Mol. Phys.*, 7, 269 (1963); 9, 301 (1965).
(26) R. S. Mulliken, C. A. Rieke, and W. G. Brown, *J. Amer. Chem. Soc.*, 63, 41 (1941).
(27) D. Peters, *J. Chem. Soc.*, 3026 (1965).

From this point of view, the OPT and MBLD barriers are seen to have a common origin; namely, each is due to a one-electron, two-center interference effect involving the CH orbital in which the part of the orbital localized near the bond hydrogen interferes with that portion of the same orbital localized near the vicinal hydrogens, and this interference favors the staggered conformation. The importance of the total change in β among nonbonded hydrogens as regards the barrier has also been observed in CNDO calculations.[7,17] Again, it is emphasized that these effects could not occur if the orbitals were truly confined to two centers; *i.e.*, they are due to an overflow of electrons onto centers outside the bond.

It is of interest to compare the INDO results with the *ab initio* calculation of the barrier by Pitzer.[15] Explicit calculation of the *ab initio* interference energies gives

$$\Delta\beta_1(2, 8) = 49.1 \times 10^{-4} \text{ au}$$

$$\Delta\beta_1(2, 6) + \Delta\beta_1(2, 7) = -41.9 \times 10^{-4} \text{ au}$$

Thus, changes in the interference energies among vicinal hydrogens within the CH bonds (ΔI) give rise to a contribution to the barrier of 43.1×10^{-4} au in the *ab initio* calculation. This amounts to about 83% of the barrier. In this case it is possible to separate the kinetic energy and electron-nuclear attraction energy contributions to ΔI. One then finds

$$\Delta I(\text{nuclear attraction}) = -40.0 \times 10^{-4} \text{ au}$$

Thus, we conclude that *all barriers* (MBLD, OPT, and *ab initio*) *are primarily due to a two-center interference electron–nuclear attraction within the CH orbital in which the part of the orbital localized near the bond hydrogen interferes with the "tails" of the same orbital on the vicinal hydrogen; this effect favors the staggered isomer.*

It is interesting to note that in the *ab initio* calculations, the one-electron overlap energy part of the interference term, ΔI, is approximately equal to the total barrier. This result implies that that part of the interference energy neglected by INDO opposes the barrier.

Hyperconjugation. Lowe[28] has recently suggested an explanation for the ethane barrier in terms of the delocalized canonical molecular orbital (CMO) representation. He found that the doubly degenerate pairs of CMO's corresponding, respectively, to pseudo-π bonding (more stable in eclipsed isomer) and pseudo-π antibonding (more stable in staggered isomer) were largely responsible for the barrier, the nondegenerate CMO's being unimportant. By then considering the methyl groups as hyperconjugative extensions of the molecule, he deduced that staggered ethane is preferred for the same reason *trans*-butadiene is preferred.[29] Since, in analogy to our discussion, his arguments also involve interactions between hydrogen 1s functions at opposite ends of the molecule, one might wonder if these delocalized results are traceable to their localized analogs.[30]

This indeed turns out to be the case, for we find that λ_1 contains no contributions from the degenerate orbitals in either of our calculations, while

$$\lambda_1 = (1/\sqrt{3})[\bar{A} + E + E'] \quad (34)$$

in all cases. Here, $\bar{A}$ is a linear combination of the nondegenerate CMO's, E is a linear combination of the two degenerate pseudo-π bonding CMO's, and E' is a linear combination of the two degenerate pseudo-π antibonding CMO's. For the OPT case, we have

$$\bar{A} = \pm(0.5457)A - (1/\sqrt{2})A' - (0.4494)A'' \quad (35)$$

while for MBLD

$$\bar{A} = \pm(0.5667)A - (1\sqrt{2})A' - (0.4228)A'' \quad (36)$$

with the plus (minus) sign taken for the staggered (eclipsed) isomer. The A, A', and A'' represent respectively, the lowest, intermediate, and highest of the previously mentioned nondegenerate CMO's found by Lowe to be unimportant for the barrier. We see, then, that the hyperconjugate effects he observed will appear only in our localized CH orbitals.

The interference energy from the "tails" can be written

$$\Delta\beta_1(2, \text{vicinal H's}) = \Delta\beta_A(2, \text{vicinal H's}) + \Delta\beta_D(2, \text{vicinal H's}) \quad (37)$$

where $\Delta\beta_D(2, \text{vicinal H's})$ is the contribution due to the functions E and E'. It follows from (34) that $\Delta\beta_D$ arises only from the *changes* in the pseudo-π bonding and antibonding CMO's which accompany the internal rotation, and hence we have isolated the portion of the interference energy $\Delta\beta_1(2, \text{vicinal H's})$ which corresponds to *changes* in the hyperconjugation of the degenerate orbitals. We find for both OPT and MBLD that $\Delta\beta_D(2, \text{vicinal H's})$ is about 70% of $\Delta\beta_1(2, \text{vicinal H's})$ and hence about 70% of the barrier: *the hyperconjugate* interpretation of Lowe[28] using the CMO's is largely equivalent to our LMO description in terms of "tails."

In view of the connection between the "tails" and hyperconjugate effects,[25,27] we should not expect the former to be due to the orthogonality of the LMO's. Presently we shall demonstrate, at least in a sense, that this is indeed the case. To this end we take the MBLD results and require the bonds to be perfectly two-center by zeroing all coefficients of basis functions not on the bonded atoms. These "bond functions" are then symmetrically orthonormalized[31] for the staggered rotamer with the INDO metric. Since the eclipsed orbitals differ from those of the staggered conformation only in the "tails" (see Table II), the same set of "bond functions" would be obtained if the eclipsed isomer were used. The orbitals appear in Table VII and the overflow is quite different in the CH orbital, *there being no "tails" on the vicinal hydrogens.* Thus, we see that even if we start with two-center bond functions having very nearly the same bond polarity as our LMO's, and then symmetrically orthonormalize[31] them, we do not obtain approximations to the LMO's which have the proper "tails." In this sense, we say that the "tails" do not appear merely because of orthogonality requirements (the orthonormal bond functions satisfy these requirements, yet have much smaller "tails"), but have some

(28) J. P. Lowe, *J. Amer. Chem. Soc.*, **92**, 3799 (1970).
(29) R. Hoffmann and R. A. Olofson, *ibid.*, **88**, 943 (1966).
(30) In fact, this did not occur to us; we are grateful to an anonymous referee who suggested the possible connection.
(31) P. O. Löwdin, *J. Chem. Phys.*, **18**, 365 (1950).

Table VII. Orthonormal Bond Functions in Ethane[a]

Atomic orbitals	MBLD 1	MBLD 4
$C_1(2s)$	0.3518	0.3691
$C_1(2p_x)$	0.5660	0.0000
$C_1(2p_y)$	0.0000	0.0000
$C_1(2p_z)$	−0.2153	0.6031
H_2	0.7137	0.0000
H_3	−0.0070	0.0000
H_4	−0.0070	0.0000
$C_5(2s)$	0.0000	0.3691
$C_5(2p_x)$	0.0000	0.0000
$C_5(2p_y)$	0.0000	0.0000
$C_5(2p_z)$	0.0000	0.6031
H_6	0.0000	0.0000
H_7	0.0000	0.0000
H_8	0.0000	0.0000

[a] Units are $(\text{bohr})^{-3/2}$.

physical basis. We shall study them further in connection with bond properties in a forthcoming paper.

V. Conclusion

The two sets of INDO calculations are similar in that (1) both predict essentially the same total barrier; (2) both predict that the change in the quasiclassical two-center attraction energy approximately cancels the sum of the changes in the electron and core repulsion energies; and (3) both reveal the barrier as being due to changes in the one-electron two-center interference energy between the bond hydrogen and its vicinal hydrogens within a CH bond and, in particular, to a change from constructive interference between the bond and trans hydrogens in the staggered conformation to destructive interference between the bond and cis hydrogens in the eclipsed conformation. The more emphatic differences encountered in the analysis of the energy terms are as follows. (1) OPT predicts that the total core and electron repulsion energies favor the eclipsed conformation, and the total quasiclassical two-center attraction energy favors the staggered isomer, while MBLD makes exactly the opposite prediction. (2) OPT predicts that the CC bond energy actually changes more than that of a single CH bond and in the opposite direction, this change being due to increased 2s character on the carbon cores in the eclipsed conformation. On the other hand, MBLD predicts a rather small change in the CC bond energy, this change being in the same direction as that of the CH bonds. Thus, even when geometry optimization has little effect on the internal rotation barrier, it can nonetheless have important consequences for the interpretation of the barrier.

In view of the similarities between the present results and those of the *ab initio* calculations,[15,22] we contend that any description of the barrier to internal rotation in ethane which assumes that the electron or nuclear repulsion energy favors the staggered form or that the CC bond is virtually unchanged may be unrealistic. Similarly, the two-center quasiclassical attraction energy should favor the staggered rotamer, and changes in this quantity should largely cancel changes in the two repulsion energies.

A similar analysis performed on geometry-optimized *ab initio* ethane wave functions may be of interest. In addition to the partitioning employed in the present work, it would then be possible to undertake a complete inter- and intraorbital partitioning as outlined in section I, as well as to investigate such properties as the kinetic energy and one-center attraction energies.

As we mentioned in the introductory section, we feel that physical, or qualitative, ideas should accompany barrier analyses. We also feel that the present work demonstrates the possibility of pursuing this with semiempirical wave functions and, as Lowe[28] mentions, we are of the opinion that these methods may be more transparent than *ab initio* calculations. Furthermore, we believe that semiempirical and *ab initio* methods can and should be used to exploit their mutual advantages in subservience to the goal of a realistic and broad physical understanding.

Finally, the type of analysis presented in this work may also be useful for other barriers and phenomena such as keto–enol tautomerism and strain energies in cyclic systems.

Acknowledgment. The authors are indebted to Professor Klaus Ruedenberg for reading the manuscript prior to publication. We are also indebted to a referee for several very constructive suggestions.